Materials Science & Engineering A 601 (2014) 70–77

Contents lists available at ScienceDirect

Materials Science & Engineering A

journal homepage: www.elsevier.com/locate/msea

Effects of substituting ytterbium for scandium on the microstructure and age-hardening behaviour of Al–Sc alloy

N.Q. Tuan [a,*], A.M.P. Pinto [a], H. Puga [a], L.A. Rocha [a,b], J. Barbosa [a]

[a] CT2M – Centre for Mechanical and Materials Technologies, University of Minho, Azurém, 4800-058 Guimarães, Portugal
[b] Universidade Estadual Paulista (Unesp), Faculdade de Ciências de Bauru, SP 17033-360, Brazil

ARTICLE INFO

Article history:
Received 11 December 2013
Received in revised form
12 February 2014
Accepted 14 February 2014
Available online 20 February 2014

Keywords:
Aluminium–scandium alloys
Ytterbium
Age-hardening
Precipitate coarsening
TEM
High-resolution TEM

ABSTRACT

In order to reduce the cost of Al–Sc alloys and maintain their mechanical properties, the microstructure and mechanical properties of Al–0.24 wt% Sc–0.07 wt% Yb in comparison with Al–0.28 wt% Sc alloys were studied. The aging behaviour, precipitate morphologies, precipitate coarsening and precipitation hardening of both alloys were investigated. The average diameter and the size distribution of nanoscale Al_3Sc and $Al_3(Sc,Yb)$ precipitates at various aging conditions were measured. Transmission electron microscopy (TEM) and high-resolution TEM were used to deeply understand the precipitate evolution. A maximum hardness around 73 (HV_{30}) was obtained with a precipitate diameter from 4.3 to 5.6 nm for both alloys.

1. Introduction

Al–Sc alloys have excellent mechanical properties at ambient and elevated temperatures due to the presence of a high number density (as high as $10^{22}\,m^{-3}$) of elastically-hard Al_3Sc ($L1_2$ structure) precipitates [1–4]. The Al_3Sc precipitates remain fully coherent with the α-Al matrix at elevated temperatures [1,5]. Among alloying elements of Al alloys, Sc has one of the greatest strengthening effects on a per-atom basis [6]. The Al_3Sc precipitates are very stable with respect to coarsening, even for long aging times at 350 °C [1], while in commercial age-hardening 2xxx and 6xxx series alloys containing Cu, Mg and Si, the precipitates coarsen rapidly at temperatures above 250 °C [6]. At ambient temperature the lattice parameters of Al and Al_3Sc are 0.40496 and 0.4105 nm, respectively, showing a small lattice parameter mismatch of Al_3Sc precipitates with the α-Al matrix [7–9]. A good interfacial strength between the Al_3Sc precipitates and the α-Al matrix will hinder dislocation motion and prevent grain growth [10]. In addition, the high thermal stability of the Al_3Sc precipitates will improve the strength of these alloys at high temperature [11,12]. Therefore Al–Sc alloys are widely used in the fabrication of sports equipment, aerospace components and in a range of structural applications.

Although Al–Sc alloys are very attractive, their use is limited by the cost and availability of Sc. A possible solution for this problem could be replacing part of the Sc content by other alloying elements similar in nature in order to reduce the Sc content without decreasing properties. Among them, rare-earth metals (REMs) are attractive ternary additions to substitute Sc, showing some interesting characteristics/benefits: (i) many REMs substitute Sc in the Al_3Sc precipitates forming $Al_3(Sc_{1-x}REM_x)$ ($L1_2$ structure) with high solubility [13,14]; (ii) the light REMs have a smaller diffusivity in Al than Sc [15], improving the coarsening resistance of the precipitates; (iii) REMs increase the lattice parameter mismatch between α-Al and $Al_3(Sc_{1-x}REM_x)$ [13,14], which could increase the creep resistance of the alloy [16]; (iv) most of the REMs have electronegativity values very similar to Sc suggesting that these metals should strongly resemble Sc in their interaction with α-Al. The metallic radii of all REMs are significantly larger than Sc leading to an increasing of the lattice parameter mismatch between α-Al and $Al_3(Sc_{1-x}REM_x)$. Karnesky et al. [17] showed that the Vickers hardness of Al–0.06 at% Sc–0.02 at% REM alloys (REM = Dy, Er, Gd, Sm, Y, or Yb) aging at 300 °C are generally similar to that of Al–0.08 at% Sc alloy. The Al–0.06 at% Sc alloys microalloyed with Yb or Gd have much improved creep resistance when compared to binary Al–Sc or ternary Al–Sc–Zr alloys with the same composition and precipitate radius [18]. According to Sawtell and Morris [19,20], addition of 0.3 at% Er, Gd, Ho, or Y improves the tensile strength of Al–0.3 at% Sc alloys at room temperature.

* Corresponding author. Tel.: +351 253510220; fax: +351 253516007.
E-mail address: quoctuan1884@gmail.com (N.Q. Tuan).

http://dx.doi.org/10.1016/j.msea.2014.02.042
0921-5093

In this study, we investigate dilute Al–0.24 wt% Sc alloys with microalloying addition of 0.07 wt%Yb to compare with Al–0.28 wt %Sc alloy. The effects of substituting Yb for Sc on the microstructure and the mechanical properties of Al–Sc alloy are investigated by using SEM, TEM, high-resolution TEM and Vickers hardness.

2. Experimental procedure

Al–0.28 wt% Sc and Al–0.24 wt% Sc–0.07 wt% Yb alloys were cast by using commercially pure Al (99.83 wt% purity), Al–2 wt% Sc master alloy and pure Yb (99.99 wt% purity). The alloys were melted in a graphite crucible using a high frequency induction furnace. For each alloy, pure Al was firstly melted at 720 °C ± 5. Then the Al–2 wt% Sc master alloy and pure Yb were added into the melt. The melt was kept at this temperature for 30 min and stirred with an alumina rod to ensure homogeneity. The molten alloys were poured into cylindrical copper moulds with 16 mm in diameter and 80 mm in length and water cooled. The composition of the as-cast alloy was measured by X-ray Fluorescence Spectrometry (Bruker S8 Tiger). The chemical composition of the as-cast alloys is given in Table 1.

In order to study the effect of homogenization treatment and aging temperature on precipitation behaviour and age hardening response, two separate studies were conducted: in one, the as-cast alloys were treated at 640 °C for 72 h for homogenization and water quenched to room temperature. The samples were subsequently treated at various temperatures within the range 150–375 °C for 2 h, followed by water quenching to ambient room temperature; in the other, the same procedure without homogenization treatment was carried out.

In order to evaluate the aging kinetics, isothermal aging without homogenization treatment of the cast samples was carried out. The samples were aged at different temperatures between 300 and 350 °C for times ranging from 10 min to 7 days.

Vickers hardness was used to monitor the hardening behaviour. Vickers hardness measurements were performed at room temperature using 30 kg load and 20 s dwell time. Eight measurements were performed on each sample. Scanning electron microscopy (SEM) micrographs were obtained on a Nano-SEM-FEI Nova 200 FEG/SEM scanning electron microscope. Transmission electron microscopy (TEM) and high resolution electron microscope (HRTEM), were used to determine the structure and morphological characteristics of the precipitates. The specimens were examined by FEI TECNAI G20 operating at 200 kV. Thin foils for transmission electron microscope (TEM) and high resolution electron microscope (HRTEM) observations were sectioned from the alloys under different conditions. The foils were prepared by double-jet electropolishing in a solution of 25% nitric acid and 75% methanol solution. In order to determine the average diameter and evaluate the number of precipitates, the TEM micrographs were analysed by Image J software. For each condition, four TEM micrographs at various positions of sample with more than 200 precipitates were selected to measure the precipitate size.

3. Results and discussion

3.1. Age hardening behaviour of the as-cast alloys

3.1.1. Effect of homogenization treatment and aging temperatures on ageing behaviour

The Vickers hardness curves of Al–0.28 wt% Sc and Al–0.24 wt% Sc–0.07 wt% Yb alloys aged at various temperatures within the range 150–375 °C for 2 h with and without homogenization treatment are shown in Fig. 1. It is evident that the hardness values of the alloys aged in the as-cast condition are significantly higher than those of the alloys homogenized and aged. In the as-cast alloys, Sc and Yb exist in α-Al supersaturated solid solution due to the high cooling rate during solidification. The precipitation of intermetallic particles occurs during the homogenization treatment, reducing the supersaturation level of Sc and Yb in α-Al solid solution. As a consequence, homogenized alloys will have the lower hardening effect due to the lower fraction volume/density of precipitates. Fig. 2 shows SEM micrographs of as-cast and homogenized Al–0.24 wt% Sc–0.07 wt% Yb samples. In the homogenized samples, several large particles of intermetallic precipitates were formed and heterogeneously distributed in α-Al.

Also shown in Fig. 1 is the effect of substituting 0.07 wt% Yb for Sc of Al–0.28 wt% Sc alloy on aging behaviour at various temperatures. The onset of age hardening for both alloys occurs at 200 °C. The precipitates form most rapidly at the temperature range of 300–350 °C, for which the highest hardness values were obtained. In the aging process without homogenization treatment, the Vickers hardness value peaks of Al–0.28 wt% Sc and Al–0.24 wt% Sc–0.07 wt% Yb alloys are 72 HV at 325 °C and 68 HV at 350 °C, respectively. A decreasing in Vickers hardness is observed for both alloys for temperatures higher than 375 °C due to the precipitate

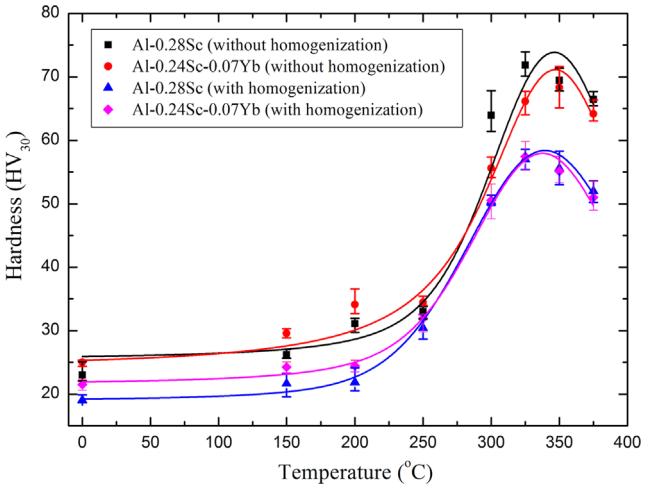

Fig. 1. Vickers hardness curves of Al–0.28 wt% Sc, Al–0.24 wt% Sc–0.07 wt% Yb alloys at various aging temperatures with and without previous homogenization treatment.

Table 1
Chemical composition of the as-cast alloys.

Alloy	Sc	Yb	Si	Fe	Ni	Cu	Ba	Mn	Ti	Al
Al–Sc										
wt%	0.283	–	0.383	0.130	0.010	0.007	0.060	0.010	0.009	Bal
at%	0.170		0.369	0.063	0.005	0.003	0.012	0.005	0.005	Bal
Al–Sc–Yb										
wt%	0.243	0.068	0.328	0.208	0.040	0.032	0.015	–	–	Bal
at%	0.146	0.011	0.316	0.101	0.018	0.014	0.003	–	–	Bal

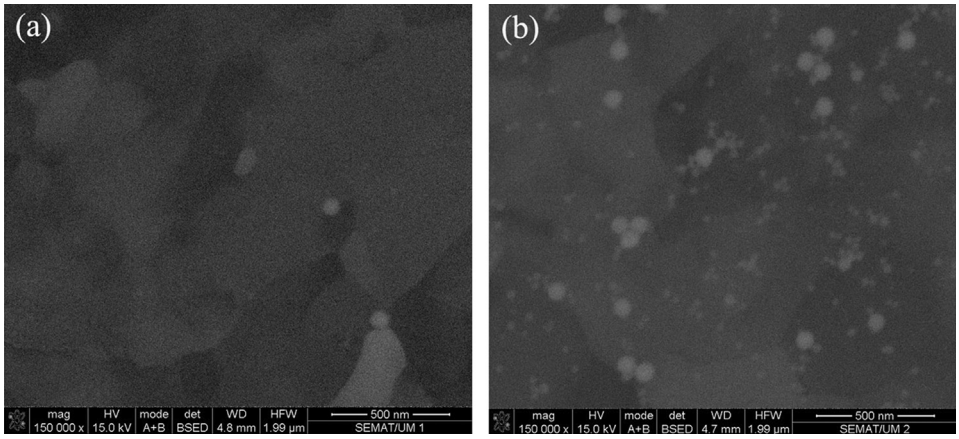

Fig. 2. SEM micrographs of Al–0.24 wt% Sc–0.07 wt% Yb alloy: (a) as-cast and (b) homogenization treated.

coarsening. The results showed that the partial replacement of Sc by Yb did not significantly affect either the kinetics or the peak hardness. Karnesky et al. [17] reported similar effect of Yb on the hardening response of an Al–0.08 at% Sc based alloy.

The alloys used in this work present in their composition small contents of other elements, namely Si and Fe that may have some small influence on the alloys mechanical properties, namely hardness. Nevertheless, the difference between both alloys is very small, suggesting that the relative hardness values have not been influenced by the presence of those elements.

3.1.2. Isothermal aging behaviour

The age hardening behaviour of Al–0.28 wt% Sc and Al–0.24 wt % Sc–0.07 wt% Yb alloys at aging temperatures of 300, 325 and 350 °C is shown in Fig. 3. It is quite evident that the Al–0.24 wt% Sc–0.07 wt% Yb alloy shows the similarity of Vickers hardness and aging behaviour with the Al–0.28 wt% Sc alloy. All the curves exhibits four different regions: (a) an incubation period; (b) a period with a rapid increase in hardness values where the precipitates nucleate from a supersaturated solid solution and grow; (c) a period of maximum hardness values (peak aging); and (d) over-aging, characterized by a slow decrease in hardness by the precipitates coarsening. The time to reach the hardness value peak decreases when the aging temperature increases from 300 to 350 °C. The Al–0.28 wt% Sc and Al–0.24 wt% Sc–0.07 wt% Yb alloys reach the hardness value peak after 20, 5, and 1 h when aging at 300, 325, and 350 °C, respectively. Higher temperature leads to earlier occurrence of over-aging. In Fig. 3(a), there is no significantly softening due to over-aging for both alloys aged at 300 °C after 7 days. However, Fig. 3(b) and (c) shows a fast over-aging for both alloys aged at 325 and 350 °C. At these aging temperatures, the hardness drop becomes obviously after reaching the peak values. Higher aging temperature conducts to higher diffusion rate for precipitates nucleation and growth. It accelerates the over-aging stage.

3.2. Evolution of precipitates

3.2.1. Precipitate morphologies

The aging behaviour presented above is controlled by the alloys microstructure. In order to correlate the observed hardening with microstructures, TEM and HRTEM observations were performed on samples at different processing states to reveal the evolution of the precipitates.

The TEM micrographs of Al–0.28 wt% Sc and Al–0.24 wt% Sc–0.07 wt% Yb alloys aged at 325 °C for 5 h, 325 °C for 7 days, and 350 °C for 7 days are shown in Fig. 4, respectively. In order to observe more clearly the morphology of precipitates, higher magnification of TEM micrographs with bright-field and dark-field techniques are exhibited in Fig. 5. The micrographs show the approximately spheroidal Al_3Sc and $Al_3(Sc,Yb)$ precipitates, uniformly distributed throughout the α-Al matrix. The $Al_3(Sc,Yb)$ precipitates in Al–0.24 wt% Sc–0.07 wt% Yb alloy could be Al_3Sc, $Al_3(Sc_{1-x}Yb_x)$ (Sc-rich composition), $Al_3(Yb_{1-x}Sc_x)$ (Yb-rich composition), or Al_3Yb precipitates. There are no signs of coherency loss that can be observed in Figs. 4 and 5. The precipitates in both alloys aged at the higher temperature (350 °C) for long holding time (7 days) still remain coherent with α-Al matrix. The precipitate diameter of both alloys at the different aging conditions was measured and the corresponding results are presented in Table 2. After aging at 300 °C for 7 days the average diameter of Al_3Sc precipitate is 5.6 nm and that of $Al_3(Sc,Yb)$ precipitate is 5.9 nm. The presence of very small precipitates after long aging time indicates that coarsening occurred very slowly at 300 °C. In combination with hardness results presented in Section 3.1, it can be seen that the strongest hardening effects of both alloys was achieved at aging temperature of 300 °C. When alloys were aged at 325 °C, the average diameter is 4.3 nm for the Al_3Sc precipitate and 4.5 nm for the $Al_3(Sc,Yb)$ precipitates at the aging peak. With prolonged aging times, after 7 days the average diameter of Al_3Sc and $Al_3(Sc,Yb)$ precipitates slowly increase to 8.4 and 8.8 nm, respectively. At the temperature of 350 °C and 7 days aging, the average diameter of Al_3Sc and $Al_3(Sc,Yb)$ precipitates are 13.7 and 15.4 nm, respectively. The TEM images show a smaller number of larger size precipitates due to the coarsening process. The average precipitates size of Al–0.24 wt% Sc–0.07 wt% Yb alloy is slightly higher than that of Al–0.28 wt% Sc alloys for all aging conditions. Thus, it suggests that Yb did not affect the coarsening rate of Al–Sc alloy.

The precipitates size distribution (PSDs) of Al–0.28 wt% Sc and Al–0.24 wt% Sc–0.07 wt% Yb alloys aged at 325 °C and 350 °C for 7 days is illustrated in Fig. 6. The PSDs of Al–0.28 wt% Sc aged at 325 °C for 7 days showed more narrow width in comparison with Al–0.24 wt% Sc–0.07 wt% Yb alloys at the same aging condition. The precipitates diameter ranges of Al–0.28 wt% Sc and Al–0.24 wt % Sc–0.07 wt% Yb alloys are 7–10.5 and 5–12 nm, respectively. The PSDs of both alloys aged at 350 °C for 7 days exhibited a similar width. The precipitates diameter ranges of Al–0.28 wt% Sc and Al–0.24 wt% Sc–0.07 wt% Yb alloys at this aging condition are 10–18 and 12–20 nm, respectively.

Precipitates in Al–0.28 wt% Sc and Al–0.24 wt% Sc–0.07 wt% Yb alloys at aging peak and the most coarsened stage were deeply studied by HRTEM technique. The HRTEM images of both alloys

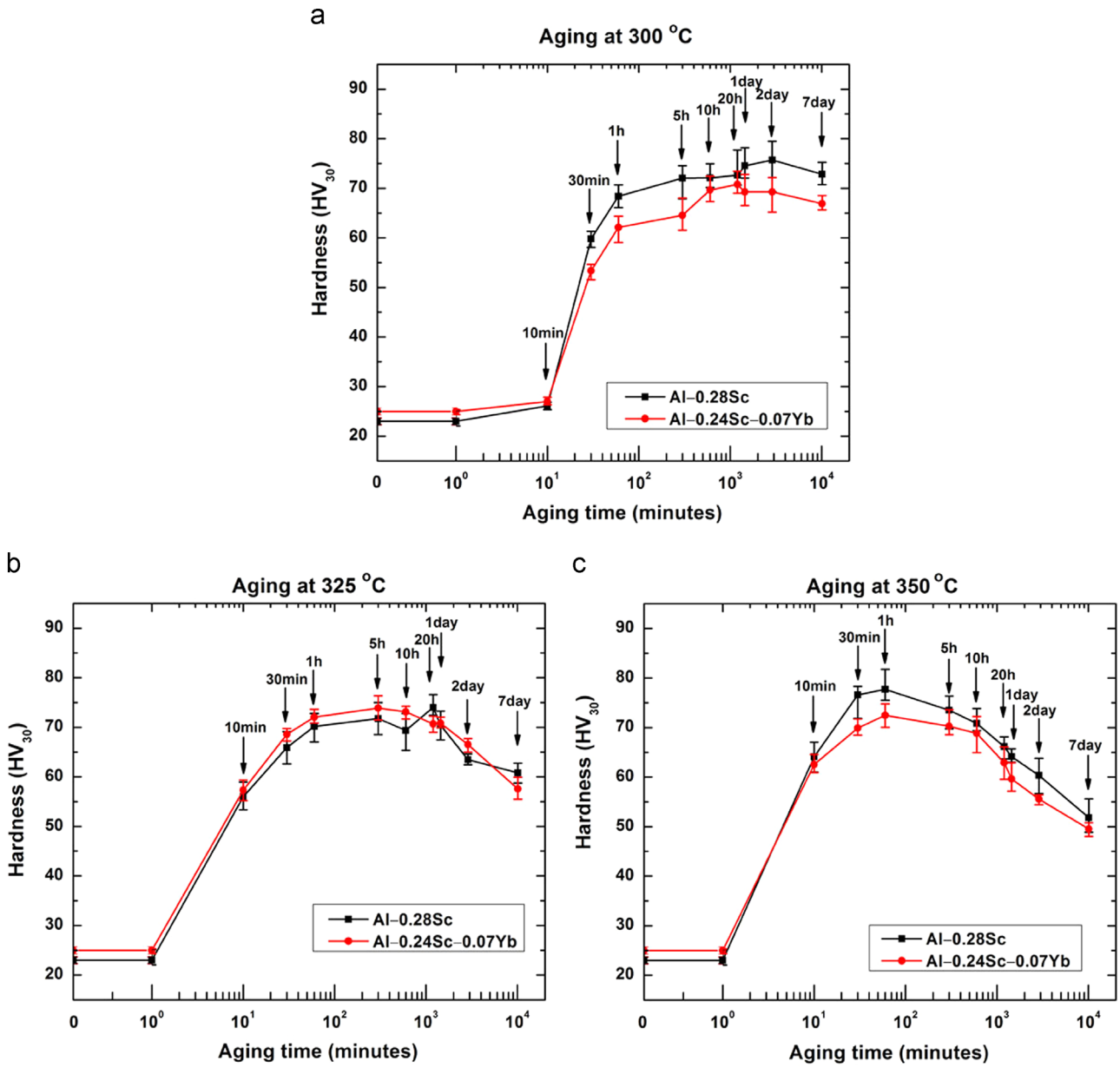

Fig. 3. Isothermal ageing curves of Al–0.28 wt% Sc and Al–0.24 wt% Sc–0.07 wt% Yb alloys at: (a) 300 °C; (b) 325 °C; (c) 350 °C.

aged at 325 °C for 5 h and 350 °C for 7 days are shown in Fig. 7. Through fast Fourier transform (FFT) analysis, the [011] zone axis orientation was found to fit well to the simulation of the reciprocal lattice section at the orientation. The FFT images show the reflections from (100) and $(0\bar{1}1)$ of Ll_2 Al_3Sc and $Al_3(Sc,Yb)$ precipitates and the reflections from (200), $(0\bar{2}2)$, and $(1\bar{1}1)$ of α-Al. The interface between the precipitates and the α-Al matrix remained coherent in both alloys even after aging at 350 °C for 7 days. There are no interfacial misfit dislocations in the HRTEM images, which conducts fully coherency of precipitates. Fig. 7 (a) and (b) shows the precipitates morphology of Al–0.28 wt% Sc and Al–0.24 wt% Sc–0.07 wt% Yb alloys aged at 325 °C for 5 h. The images show small precipitates with diameter less than 5 nm. The larger size and more obvious morphologies of precipitates are observed in Fig. 7(c) and (d) corresponding to both alloys aged at 350 °C for 7 days. The Al_3Sc precipitates in Al–0.28 wt% Sc alloy have a facetted shape that corresponds to a great rhombicubocta-hedron predicted by Marquis et al. [1]. Facets are parallel to the {100} and $\{0\bar{1}1\}$ planes. The precipitates average diameter is 18.1 nm, while the $Al_3(Sc,Yb)$ precipitate in Al–0.24 wt% Sc–0.07 wt% Yb alloy exhibits an approximately spheroidal shape with 18.5 nm diameter. The presence of Yb decreases the amount of faceting parallel to the {100} and $\{0\bar{1}1\}$ and changes the morphology of precipitates into a more spheroidal shape.

3.2.2. *Coarsening behaviour*

The coarsening behaviour of spherical precipitates in binary alloys was predicted by The Lifshitz–Slyozov–Wagner (LSW) model base on volume diffusion theory [21,22]. The Ostwald ripening of spherical precipitates was developed in concentrated multicomponent alloys by Umantsev and Olsan [23] and more detailed in ternary alloys, allowing for capillary effects by Kuehmann and Voorhees (KV) [24]. According to the KV model, the coarsening behaviour of precipitates was analysed through the

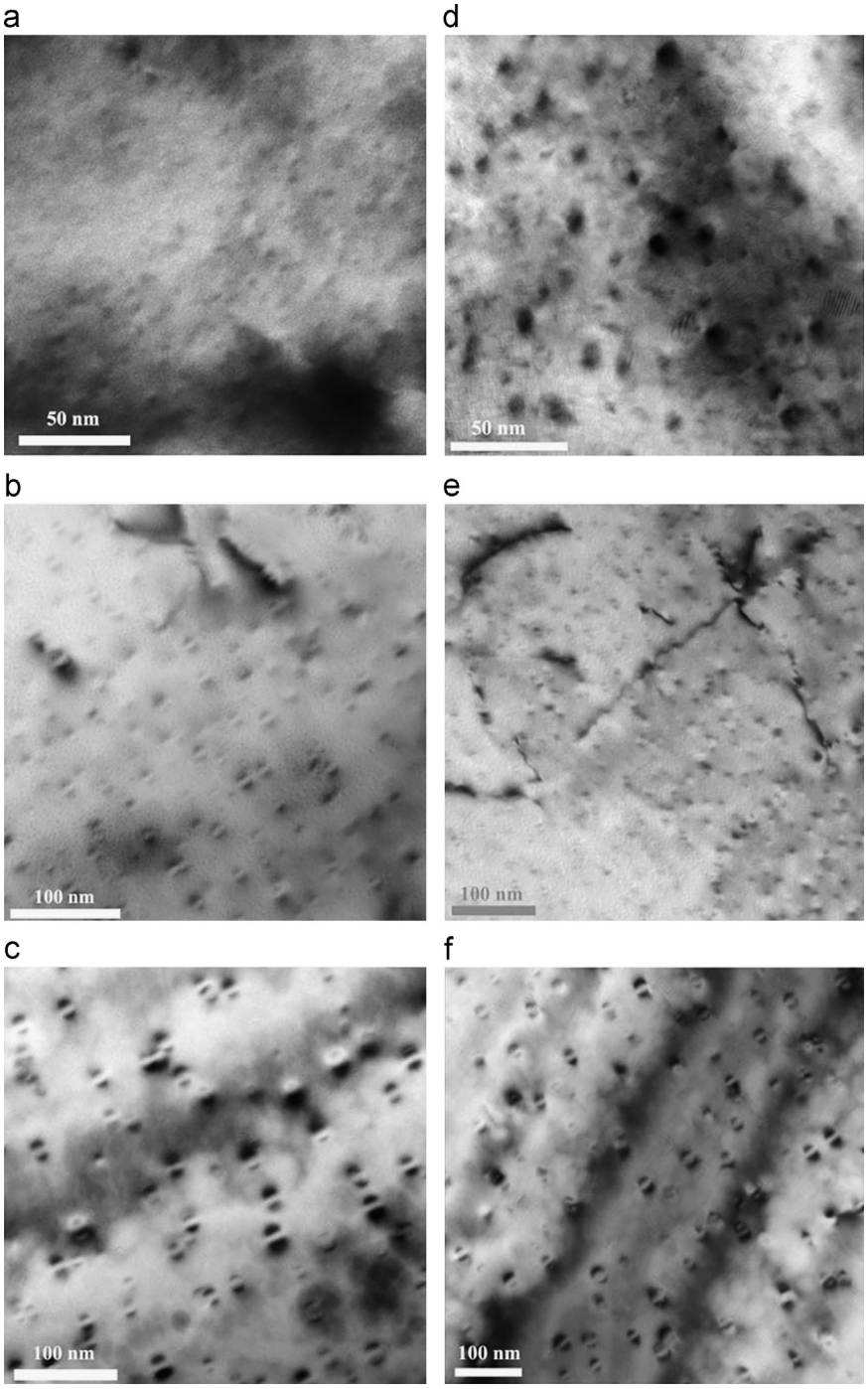

Fig. 4. TEM micrographs of Al–0.28 wt% Sc (a–c) and Al–0.24 wt% Sc–0.07 wt% Yb (d–f) alloys aged at 325 °C for 5 h, 325 °C for 7 days, and 350 °C for 7 days.

following equation:

$$\langle R(t)\rangle^n - \langle R(t_0)\rangle^n = K(t - t_0) \quad (1)$$

where K is a coarsening rate constant, $\langle R(t)\rangle$ is the average precipitate radius at time t, $\langle R(t_0)\rangle$ is the average precipitate radius at the onset of quasi-stationary coarsening at time t_0, and n is the inverse time exponent. Eq. (1) could be applied for both binary alloy (Al–0.28 wt% Sc) and ternary alloy (Al–0.24 wt% Sc–0.07 wt% Yb) with different coarsening rate constant. It was assumed that $\langle R(t_0)\rangle^n$ and t_0 is much smaller than $\langle R(t)\rangle^n$ and t, Eq. (1) became [25,26]:

$$\langle R(t)\rangle^n = Kt \quad (2)$$

A log–log plot of Eq. (2) reveals a slope of $1/n$ as following equation:

$$\log \langle R(t)\rangle = \frac{1}{n}\log t + \frac{1}{n}\log K \quad (3)$$

This slope is known as a time exponent of coarsening and often reported to indicate the coarsening behaviour of precipitates. By applying the KV model to the Al–0.28 wt% Sc and Al–0.24 wt % Sc–0.07 wt% Yb alloys aged at 325 °C, the time exponents of coarsening $1/n$ was calculated and showed the same value of 0.19 for both alloys. This value indicated that the precipitate coarsening behaviour of both investigated alloys is similar to the Al–0.18 at%

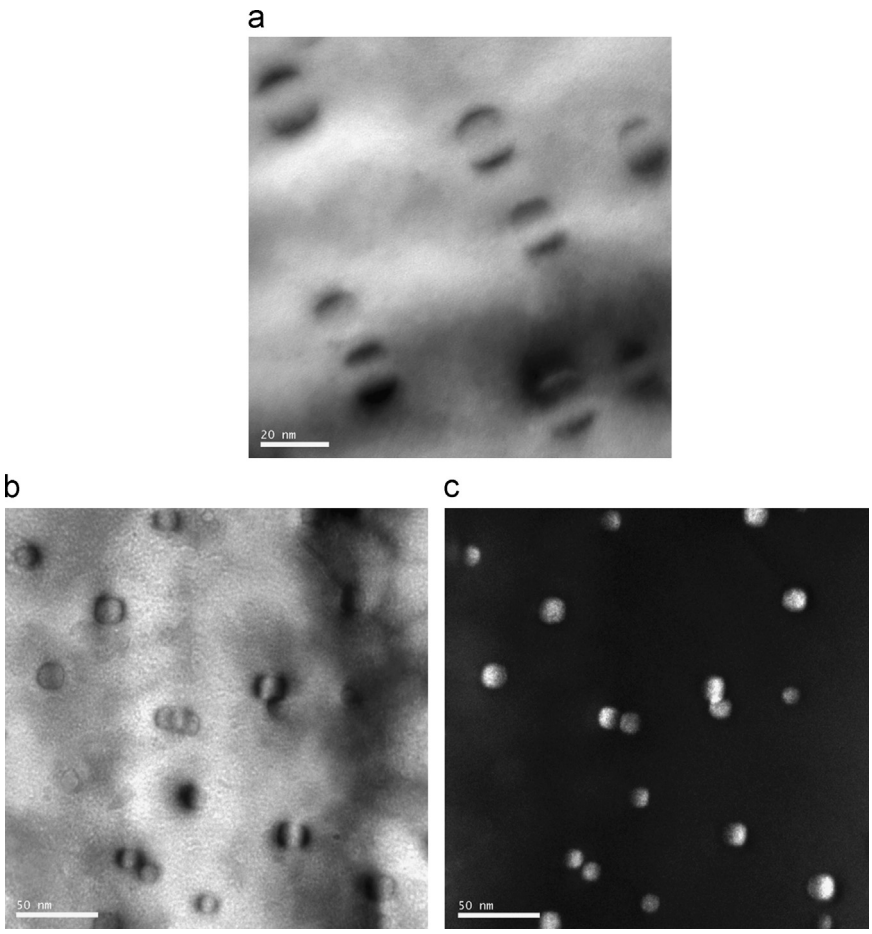

Fig. 5. TEM micrographs of Al–0.28 wt% Sc (a) and Al–0.24 wt% Sc–0.07 wt% Yb (b and c) alloys aged at 350 °C for 7 days: (a) and (b) bright-field TEM image; and (c) dark-field TEM image.

Table 2
Average precipitate diameter and hardness of Al–0.28 wt% Sc and Al–0.24 wt% Sc–0.07 wt% Yb alloys.

Aging condition	Al–0.28 wt% Sc		Al–0.24 wt% Sc–0.07 wt% Yb	
	Precipitate diameter (nm)	Hardness – HV_{30}	Precipitate diameter (nm)	Hardness – HV_{30}
300 °C, 7 days	5.6 ± 0.5	73 ± 2	5.9 ± 0.7	67 ± 2
325 °C, 5 h	4.3 ± 0.2	72 ± 3	4.5 ± 0.8	74 ± 3
325 °C, 7 days	8.4 ± 0.9	61 ± 2	8.8 ± 1.8	58 ± 2
350 °C, 7 days	13.7 ± 1.9	52 ± 3	15.4 ± 1.8	50 ± 1

Sc alloy aged at 300 °C ($(1/n)=0.18$) referred by Marquis et al. [1,25] and Al–0.06 at% Sc–0.02 at% Yb (at%) alloy aged at 300 °C ($(1/n)=0.18$) referred by Van Dalen et al. [27].

3.3. Precipitation hardening mechanisms

The evolution of precipitates and corresponding hardness at different aging conditions is presented in Table 2. According to Hyland et al. [28] and Marquis et al. [2], the volume fraction of precipitate is approximately constant for Al–Sc alloys aged at various temperatures from 275 °C to 400 °C after long enough aging time (longer than 10,000 s at 288 °C and 2000 s at 343 °C). On this work the alloys were aged at 300, 325, and 350 °C for 5 h and 7 days. For these conditions and according to the findings of Hyland and Marquis we can assume that the volume fraction of precipitates is constant. The precipitation hardening is typically understood through the cutting mechanism which dislocations cut through precipitates and the Orowan bypass mechanism which dislocations bow or loop precipitates. According to the experimental data from the study about precipitation strengthening in Al–0.3 wt% Sc alloy, Marquis et al. [2] predicted a transition from cutting mechanism to Orowan bypass mechanism at a precipitate diameter of 4.2 nm. The strength of alloy is controlled by the cutting mechanism for smaller sizes, and the Orowan bypass mechanism for larger sizes of precipitates which higher precipitate diameter results in lower hardness. Table 2 showed a maximum hardness around 73 (HV_{30}) at a precipitate diameter from 4.3 to 5.6 nm for both alloys. It sharply decreases to $HV_{30}=50$ when the average diameter of precipitate increases to 13.7–15.4 nm. This result is in a good agreement with above theory and the result of Marquis et al. [2].

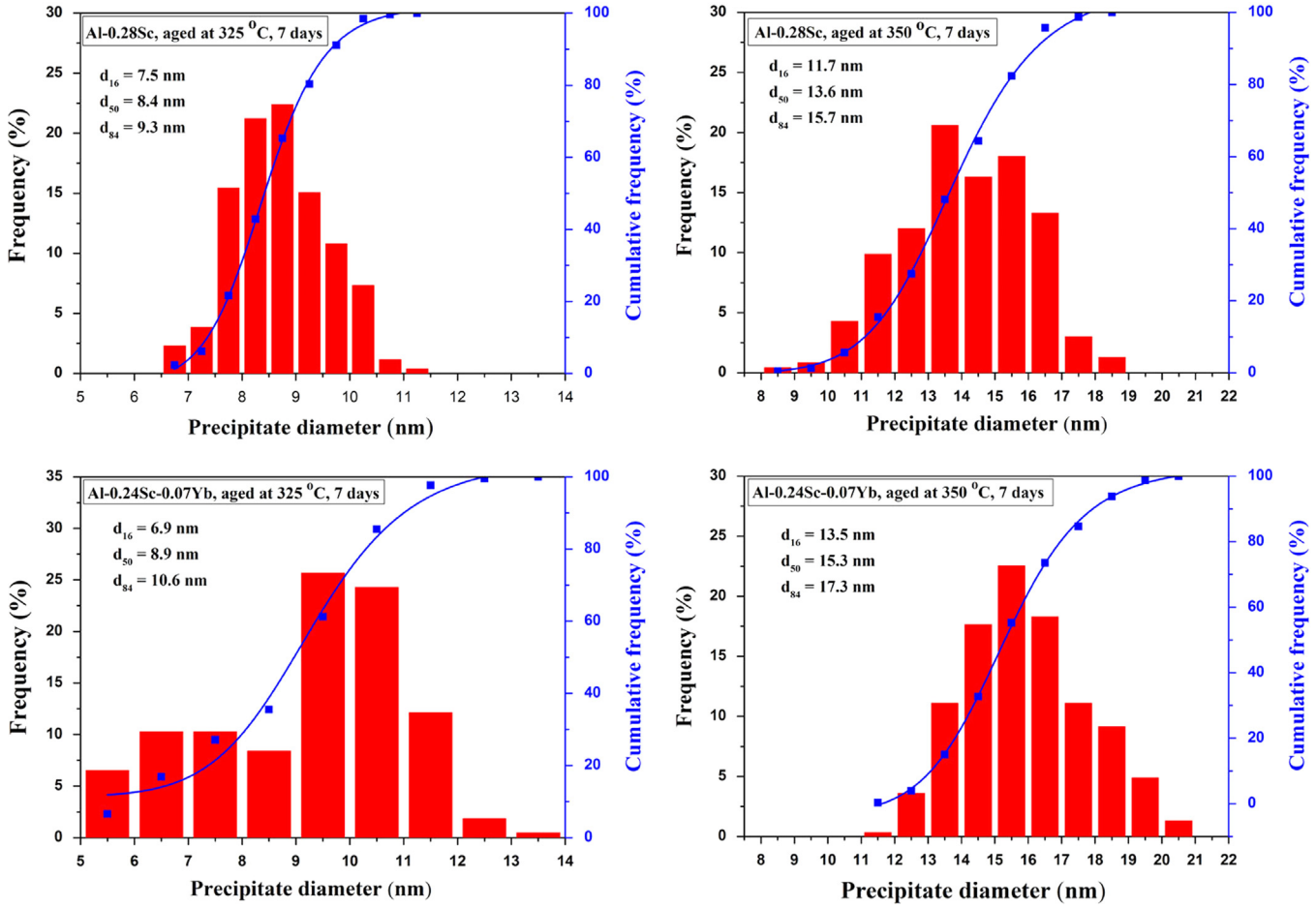

Fig. 6. Precipitates size distribution of Al–0.28 wt% Sc and Al–0.24 wt% Sc–0.07 wt% Yb alloys at different aging conditions: d_{16}, d_{50}, and d_{84} are the precipitate diameters corresponding to 16%, 50%, and 84 % cumulative undersize particle size distribution.

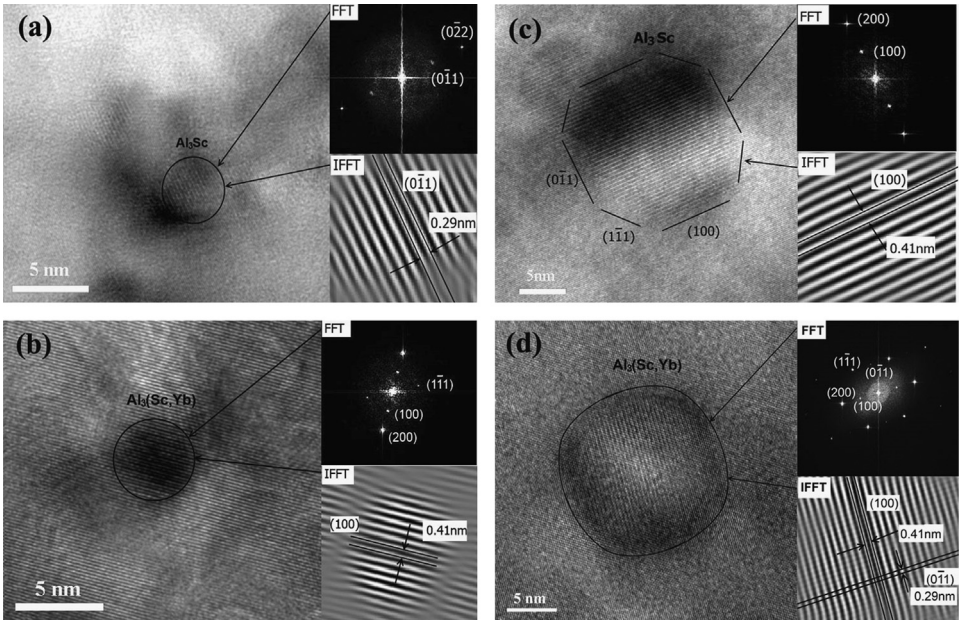

Fig. 7. High-resolution TEM images of Al–0.28 wt% Sc (a–c) and Al–0.24 wt% Sc–0.07 wt% Yb (b–d) alloys aged at 325 °C for 5 h and 350 °C for 7 days.

4. Conclusions

The similarity of microstructure, hardness and aging behaviour of Al–0.24 wt% Sc–0.07 wt% Yb alloy in comparison with Al–0.28 wt% Sc alloy was shown in this investigation. It indicates that the substitution of 0.07 wt% Yb for more expensive Sc in the Al–0.28 wt% Sc alloy is possible. Some final characteristics of Al–0.28 wt% Sc and Al–0.24 wt% Sc–0.07 wt% Yb alloys were concluded below:

- The hardness values of both alloys aged without homogenization treatment are significantly higher than those of alloys aged after homogenization treatment.
- The approximately spheroidal Al_3Sc and $Al_3(Sc,Yb)$ precipitates were uniformly distributed throughout the α-Al matrix. The precipitates remain fully coherent with α-Al matrix even after aging at high temperature for long time.
- With the aging temperature of 325 °C, the average diameter is 4.3 nm for Al_3Sc precipitates and 4.5 nm for $Al_3(Sc,Yb)$ precipitates at the aging peak. At the temperature of 350 °C and 7 days aging, the average diameter of Al_3Sc and $Al_3(Sc,Yb)$ precipitates are 13.7 and 15.4 nm, respectively
- The Al_3Sc precipitates of Al–0.28 wt% Sc alloy show the facetted shape that are similar with great rhombicuboctahedron shape. While the $Al_3(Sc,Yb)$ precipitates of Al–0.24 wt% Sc–0.07 wt% Yb alloy show an approximately spheroidal shape.

Acknowledgements

This research was supported by The Project Bridging The Gap, funded by the Erasmus Mundus External Cooperation Window Program. Acknowledgements also to the University of Minho, for the provision of research facilities

References

[1] E.A. Marquis, D.N. Seidman, Acta Mater. 49 (2001) 1909–1919.
[2] E.A. Marquis, D.N. Seidman, D.C. Dunand, Acta Mater. 51 (2003) 285–287 (Acta Mater. 50 (2002) 4021–4035).
[3] J. Røyset, N. Ryum, Int. Mater. Rev. 50 (2005) 19–44.
[4] L.S. Toropova, D.G. Eskin, M.L. Kharakterova, T.V. Dobatkina, Advanced Aluminum Alloys Containing Scandium: Structure and Properties, Gordon and Breach, Amsterdam, The Netherlands, 1998.
[5] S. Iwamura, Y. Miura, Acta Mater. 52 (2004) 591–600.
[6] M.Y. Drits, L.B. Ber, Y.G. Bykov, L.S. Toropova, G.K. Anastas'eva, Phys. Met. Metallogr. 57 (1984) 118–126.
[7] I.C.f.D. Data, Using the Powder Diffraction File, International Centre for Diffraction Data, 1996.
[8] Y. Harada, D.C. Dunand, Mater. Sci. Eng.: A 329–331 (2002) 686–695.
[9] Y. Harada, D.C. Dunand, Scr. Mater. 48 (2003) 219–222.
[10] L.S. Kramer, W.T. Tack, M.T. Fernandes, Adv. Mater. Processes 152 (1997) 23–24.
[11] M.J. Jones, F.J. Humphreys, Acta Mater. 51 (2003) 2149–2159.
[12] V. Ocenasek, M. Slamova, Mater. Charact. 47 (2001) 157–162.
[13] O.I. Zalutskaya, V.G. Kontseyoy, N.I. Karamishev, V.R. Ryabov, I.I. Zalutskii, Dopov. Akad. Nauk. Ukr. RSR (1970) 751, http://arc.nucapt.northwestern.edu/refbase/show.php?record=293.
[14] A. Palenzona, J. Less Common Met. 29 (1972) 289–292.
[15] L.F. Mondolfo, Aluminum Alloys: Structure and Properties, Butterworths, London, 1976.
[16] E.A. Marquis, D.C. Dunand, Scr. Mater. 47 (2002) 503–508.
[17] R.A. Karnesky, M.E. van Dalen, D.C. Dunand, D.N. Seidman, Scr. Mater. 55 (2006) 437–440.
[18] M.E. Dalen, D.C. Dunand, D.N. Seidman, J. Mater. Sci. 41 (2006) 7814–7823.
[19] R.R. Sawtell, J.W. Morris, Dispersion Strengthened Aluminum Alloys, TMS, Warrendale, PA, 1988.
[20] R.R. Sawtell, Exploratory alloy development in the system Al–Sc–X, University of California, Berkeley, 1988.
[21] C.Z. Wagner, Z. Elektrochem, Angew. Phys. Chem. 65 (1961) 581.
[22] I.M. Lifshitz, V.V. Slyozov, J. Phys. Chem. Solids 19 (1961) 35–50.
[23] A. Umantsev, G.B. Olson, Scr. Metall. Mater. 29 (1993) 1135–1140.
[24] C.J. Kuehmann, P.W. Voorhees, Metall. Mater. Trans. A 27 (1996) 937–943.
[25] E.A. Marquis, D.N. Seidman, Acta Mater. 53 (2005) 4259–4268.
[26] J. Lai, Z. Zhang, X.G. Chen, J. Alloys Compd. 552 (2013) 227–235.
[27] M.E. Van Dalen, D.C. Dunand, D.N. Seidman, Acta Mater. 59 (2011) 5224–5237.
[28] R.W. Hyland, Mater. Trans. A 23 (1992) 1947–1955.